

# PLATINUM-GROUP MINERAL CHARACTERIZATION IN CONCENTRATES FROM HIGH-GRADE PGE AL-RICH CHROMITITES OF KORYDALLOS AREA IN THE PINDOS OPHIOLITE COMPLEX (NW GREECE)

AUTHOR: ARGYRIOS KAPSIOTIS, TASSOS A. GRAMMATIKOPOULOS, \*BASILIOS TSIKOURAS AND KONSTANTINOS HATZIPANAGIOTOU

DEPARTMENT OF GEOLOGY, SECTION OF EARTH MATERIALS, PANEPISTIMIIOUPOLIS OF RION, UNIVERSITY OF PATRAS, PATRAS, GREECE & SGS

## ABSTRACT

The Pindos ophiolite complex, located in the north-western part of continental Greece, hosts various podiform chromite deposits generally characterized by low platinum-group element (PGE) grades. However, a few locally enriched in PPGE + Au (up to 29.3 ppm) chromitites of refractory type are also present, mainly in the area of Korydallos (south-eastern Pindos). The present data reveal that this enrichment is strongly dependant on chromian spinel chemistry and base metal sulfide and/or base metal alloy (BMS and BMA, respectively) content in chromitites. Consequently, we used super-panning to recover PGM from the Al-rich chromitites of the Korydallos area. The concentrate of the composite chromitite sample contained 159 PGM grains, including, in decreasing order of abundance, the following major PGM phases: Pd-Cu alloys (commonly nonstoichiometric, although a few Pd-Cu alloys respond to the chemical formula  $\text{PdCu}_4$ ), Pd-bearing tetraauricupride [(Au,Pd)Cu], nielsenite ( $\text{PdCu}_3$ ), sperrylite ( $\text{PtAs}_2$ ), skaergaardite ( $\text{PdCu}$ ), Pd-bearing auricupride [(Au,Pd)Cu<sub>3</sub>], Pt and Pd oxides, Pt-Fe-Ni alloys, hollingworthite ( $\text{RhAsS}$ ) and Pt-Cu alloys. Isomertieite ( $\text{Pd}_{11}\text{Sb}_2\text{As}_2$ ), zvyagintsevite ( $\text{Pd}_3\text{Pb}$ ), native Au, keithconnite ( $\text{Pd}_{20}\text{Te}_7$ ), naldrettite ( $\text{Pd}_2\text{Sb}$ ) and Rh-bearing bismuthotelluride ( $\text{RhBiTe}$ , probably the Rh analogue of michenerite) constitute minor phases. The bulk of PGE-mineralization is dominated by PGM grains that range in size from 5 to 10  $\mu\text{m}$ . The vast majority of the recovered PPGE are associated with secondary BMS and BMA, thus confirming that a sulphur-bearing melt played a very important role in scavenging the PGE + Au content of the silicate magma from which chromian

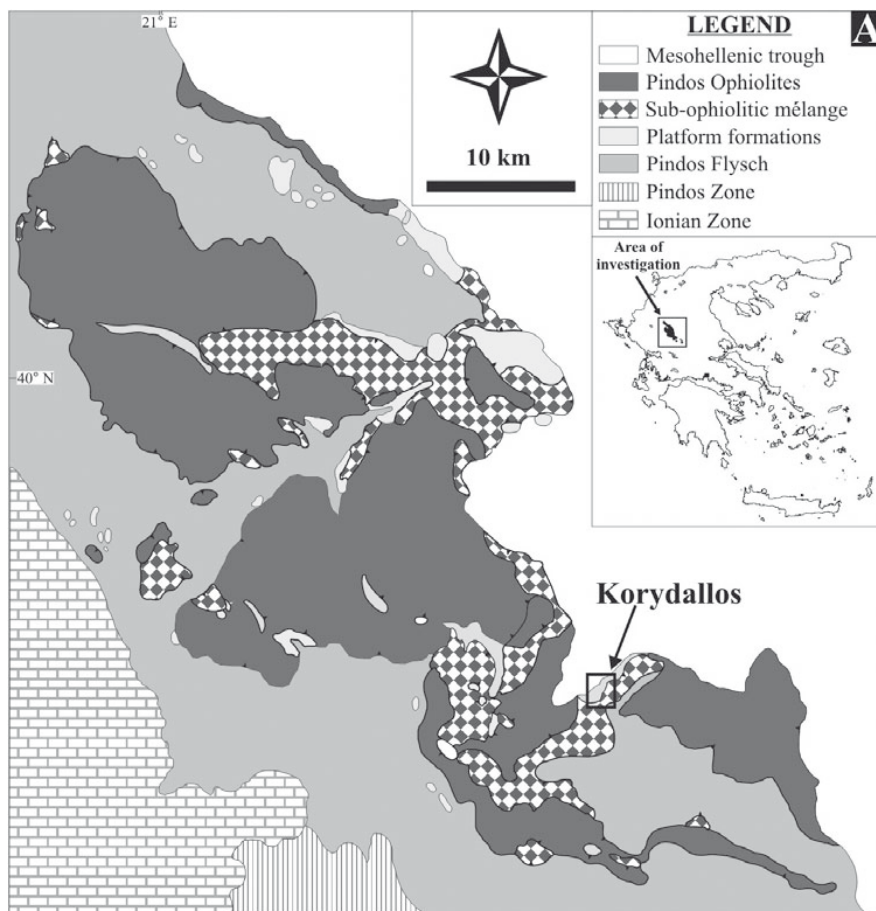
spinel had already started to crystallize. The implemented technique has led to the recovery of more, as well as noble, PGM grains than the in situ mineralogical examination of single chromitite samples. Although, the majority of the PGM occur as free particles and in situ textural information is lost, single grain textural evidence is observed. In summary, this research provides information on the particles, grain size and associations of PGM, which are critical with respect to the petrogenesis and mineral processing.

## INTRODUCTION

The study of accessory and rare minerals in rocks is limited mainly because of the low abundance and small grain size of the target minerals. The traditionally applied in situ investigation of such minerals is a useful tool for providing significant mineralogical information. However, it commonly fails to provide a complete picture of mineralogy, and thus the results cannot be considered representative. On the other hand, quantitative mineralogical studies are more statistical. In addition, new mineral species have also been recovered using such methods of investigation (e.g. Rudashevsky et al., 2004; Cabri et al., 2005a, b; McDonald et al., 2005).

In the last decades, considerable attention has been paid to the study

of ophiolitic chromitites. These can be strongly enriched in platinum-group elements (PGE), especially Os, Ir and Ru, when compared to their host rocks (e.g. Economou-Eliopoulos & Vacondios, 1995; Melcher et al., 1997; Ahmed & Arai, 2002; Zaccarini et al., 2005, 2008). In chromitites the PGE are not carried in solid solution in chromian spinel as has been proposed by experimental studies (e.g. Capobianco & Drake, 1990; Capobianco et al., 1994; Righter et al., 2004), but tend to form discrete platinum-group minerals (PGM) (e.g. Zaccarini et al., 2005; Uysal et al., 2007). Even in low-grade PGE chromitites the distribution of these elements is not homogeneous, probably due to the random occurrence, cluster and nugget effect of PGM in the chromitites. Ten chromitite samples were investigated from the area of Korydallos in the Pindos ophiolite complex, by in situ examination using both optical and scanning electron microscopy at 200–800x magnification. A systematic search yielded only four PGM grains that are not always associated with chromian spinel, and thus, failed to provide significant information of the PGE mineralogy. The discovered PGM comprised of a Pt-Fe-Ni alloy included in ferrian chromite, two skaergaardite grains attached to an awaruite grain, and a Pd-Sn phase within the silicate matrix of the chromitites. Therefore, a gravity concentration method using super-panning was implemented to better define the mineralogical assemblage of



PGE in the chromitites.

The present study provides the mineralogical results obtained on PGM grains from a concentrate from a composite sample from the podiform Al-rich chromitites of the area of Korydallos in the Pindos ophiolite complex. The aim of this paper is to demonstrate the significance of process mineralogy in characterizing the PGM-assemblage in high-grade PGE ores and/or rocks and its benefits in mainly the petrogenesis and mineral processing of these rare mineral phases.

### GEOLOGICAL SETTING

The Pindos ophiolite complex is located in northwestern Greece (Fig. 1a) and corresponds to a piece of Middle to Upper Jurassic oceanic crust (Rassios & Smith, 2000). It is tectonically emplaced over the autochthonous Maastrichtian-Eocene Pindos flysch. It is subdivided into four principal tectonic units: the Dramala complex, the

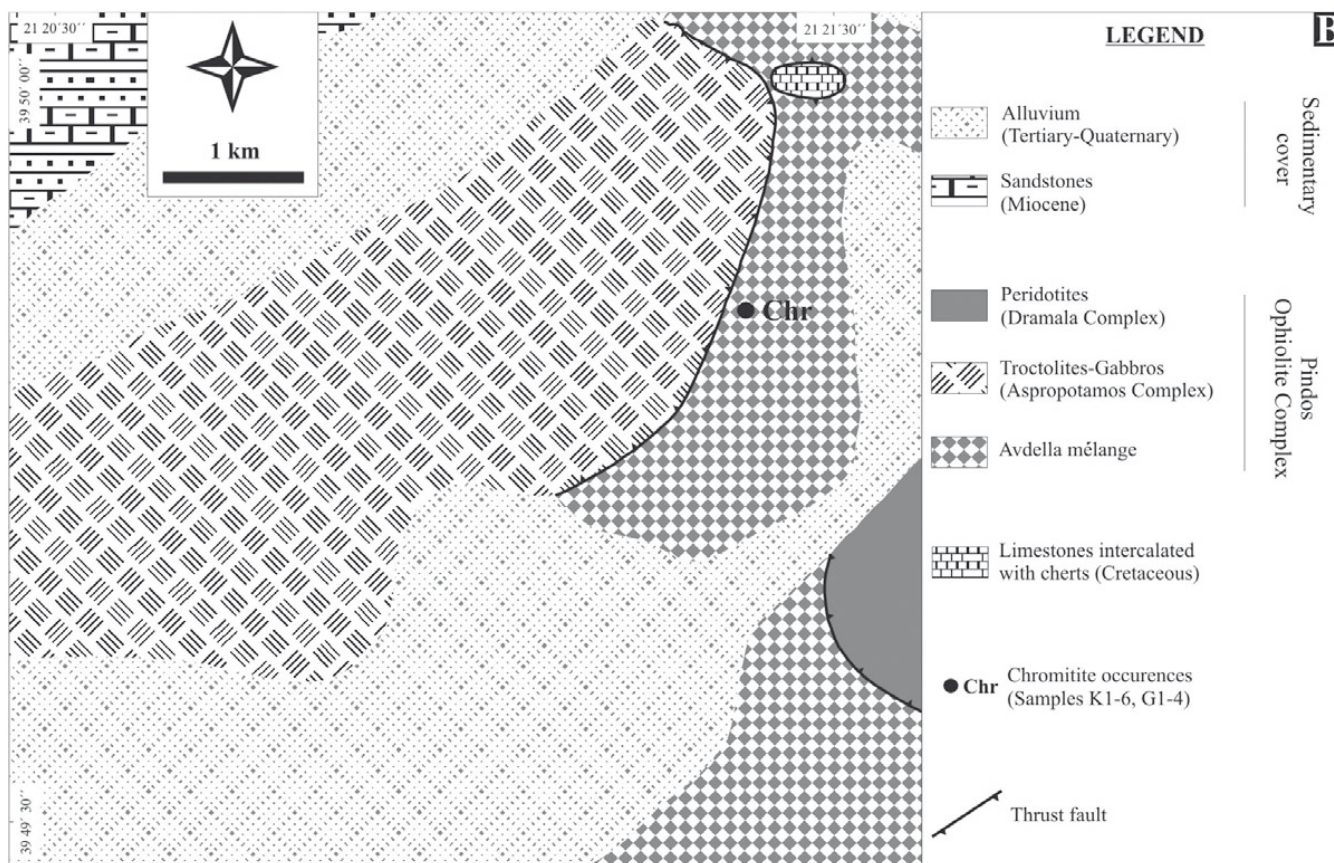


**Fig. 1** (a) Simplified geological map of the Pindos ophiolite complex showing the location of the studied area (modified after Migiros et al., 1986; Kostopoulos, 1989; Jones & Robertson, 1991) and inset map illustrating the location of the Pindos ophiolites in the Greek peninsula. (b) Detailed geologic map of the investigated area showing the location of the studied chromitites.



**Table 1** PGE and Au analyses of two chromitite samples from the area of Korydallos, showing different compositional characteristics in terms of texture, chromian spinel chemistry and noble metal abundances

Sample	Os (ppb)	Ir (ppb)	Ru (ppb)	Rh (ppb)	Pt (ppb)	Pd (ppb)	Au (ppb)	ΣPGE+ Au (ppb)	Cr#	Texture
K <sub>1</sub>	17	21	30	3.10	31	192	14.70	308.80	0.65	Disseminated
G <sub>2</sub>	266	364	2100	1140	17,100	7860	488	29,318	0.44	Massive

Loumnitsa unit and the Aspropotamos complex, all structurally lying over a chaotic lithological formation known as the Avdella mélangé (Jones & Robertson, 1991). The Dramala unit is comprised of large, variably depleted harzburgite-dunite masses (>1000 km<sup>2</sup>), which hosts small chromitite bodies (Trygona, Pefki, Milia, Korydallos, etc.) of massive, disseminated, schlieren and, less commonly, nodular texture. The crustal rocks of the Aspropotamos complex cover a wide spectrum of geochemical affinities, ranging from MORB through a mixture of MORB and IAT to IAT and finally boninitic series volcanics (BSV), which cross cut all the previous types of volcanics (Kostopoulos, 1989; Pe-Piper *et al.*, 2004). The Loumnitsa unit represents the basal metamorphic sole of both Dramala and Aspropotamos complexes, comprising low amphibolite and greenschist facies metaigneous and meta-sedimentary rocks that have yielded <sup>40</sup>Ar-<sup>39</sup>Ar ages of 169 ± 5 and 165 ± 3 Ma (Whitechurch & Parrot, 1978; Spray & Roddick, 1980). The Avdella mélangé is a chaotic mixture of about 1 km in thickness that comprises blocks of various rock types in a tectonized matrix and mappable thrust sheets (Jones & Robertson, 1991).

## TEXTURAL, MINERALOGICAL AND COMPOSITIONAL CHARACTERISTICS OF KORYDALLOS CHROMITITES

Ten representative chromitite samples were collected from the area of Korydallos (Fig. 1b), which is located in the southeastern part of the Pindos ophiolite complex. The chromitites at Korydallos are generally small, a few meters long and tens of cm in thickness. They occur as small sub-rounded shaped pods. They are disseminated or massive in texture, and are found within completely serpentized and weathered, intensively deformed dunite

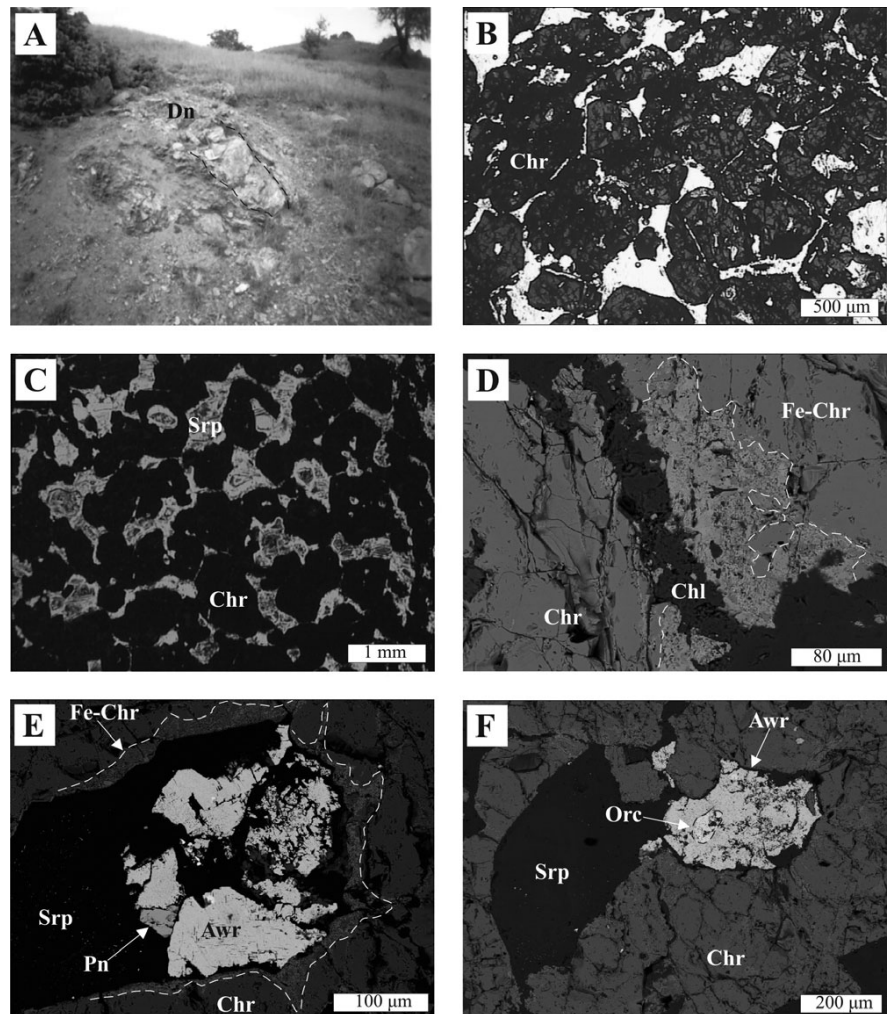


**Fig. 2** (a) Intensively deformed (mylonitized) serpentized dunite block (black dashed line) within the Korydallos mélangé. (b) Photomicrograph showing the fractured nature of brownish chromian spinels from which the Korydallos Al-rich chromitites are composed (plane polarized transmitted light). (c) Photomicrograph illustrating the complete replacement of the silicate matrix of the investigated chromite ore bodies by mesh serpentine (cross polarized transmitted light). (d) Back-scatter-electron image (SEM) showing marginal replacement of the ore hosted chromian spinel by ferrian chromite (white dashed line). (e-f) BMA and BMS crystals enclosed by chromian spinel in the Korydallos Al-rich chromitites. In picture E the marginal alteration of chromian spinel to ferrian chromite is also shown (white dashed line). Abbreviations: Dn, dunite; Chr, chromian spinel; Srp, serpentine; Fe-chr, ferrian chromite; Chl, chlorite; Pn, pentlandite; Awr, avaruite; Orc, orcelite.

blocks (Fig. 2a) included in a highly sheared, yellowish to dark green colored matrix. The chromitites are mostly fine- to medium-grained, and consist of aggregates of fractured subhedral to euhedral chromian spinel grains (Fig. 2b), whereas the interstitial matrix is composed of mesh serpentine (Fig. 2c), accompanied by chlorite and occasional traces of tremolite. Primary olivine is preserved only in the form of inclusions within chromian spinel. Chromian

spinel grains can be locally altered to ferrian chromite (Fig. 2d). Abundant remnants of base metal sulfides (BMS, now preserved as alloys) occur both as inclusions (Figs 2e, f), and interstitial phases in the silicate matrix. Locally, the presence of these metallic phases is distinguishable even in hand specimen. The composition of the ore hosted chromian spinel presents a relatively wide range in terms of Cr# [Cr/(Cr+Al)], between 0.43 and 0.69, and Mg# [Mg/

(Mg+Fe<sup>2+</sup>) 0.57 and 0.65. Their PGE + Au content varies significantly between low and extremely high. The total PGE + Au concentrations in the chromitites hosting high Cr# chromian spinel are relatively low (308.8 ppb, Table 1) and typical for ophiolitic chromitites from elsewhere (e.g. Zaccarini et al., 2005; Uysal et al., 2007). On the contrary, the total PGE + Au content in the chromitites with low Cr# chromian spinel and abundant BMS and BMA (base metal alloys) (29.318 ppm, Table 1) is one of the highest ever measured in ophiolitic chromitites worldwide, and the highest ever mentioned for chromitites from Greece. These PGE + Au concentrations are suggestive of the presence of PGM as distinct mineral phases in the investigated chromitites.

PGM recovery from low-grade PGE ophiolitic chromitites commonly leads to successful results (e.g. Kapsiotis et al., 2006; Grammatikopoulos et al., 2007; Uysal et al., 2009). However, the use of process mineralogy in characterizing the PGM assemblage in high-content PGE ores and/or rocks is important not only for petrogenetic studies but for industrial purposes as well. Thus, the recovery of PGM from the PGE enriched chromitite samples was preferred in order to increase the possibility of concentrating abundant PGM grains. Furthermore, the rich in PPGE (Rh, Pt, Pd) character of the studied chromitites, which is different from the IPGE (Os, Ir, Ru)-rich nature of most ophiolitic chromitites, provides the opportunity to complete the mineralogical characterization of the PGM species carried in these high-Al chromite ores.

## METHODS OF INVESTIGATION

Ten samples were collected from the podiform chromitites occurring at the area of Korydallos in the Pindos ophiolite complex. All the samples were collected within a radius of a few meters. Each sample was taken from two different but neighboring chromitite pods. One polished section was prepared for each sample and examined with optical and electron microscopy using a Super Jeol electron microscope (Jeol, Tokyo) at the University of Patras. The in situ

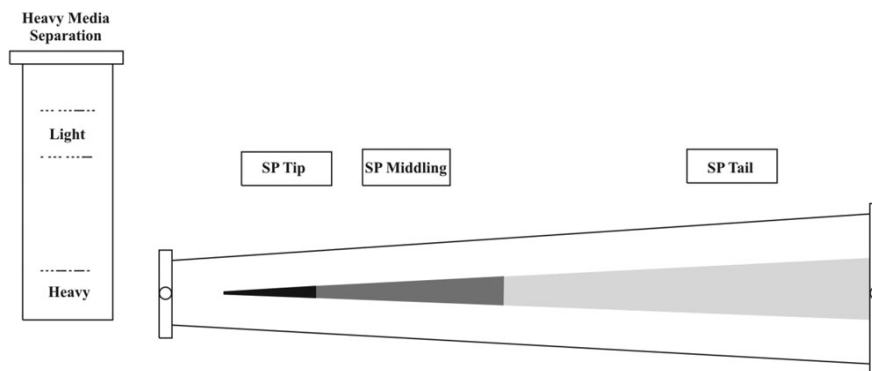


**Fig. 3** Drawn sketch explaining PGM recovery using super-panning.

examination yielded only four PGM grains. Consequently, five chromitite samples of approximately 500 g each were chosen, stage crushed at -10 mesh, blended and homogenized in order to generate a composite sample from the most Al-rich (and PPGE-enriched) chromitite samples. The composite sample was then riffled to obtain 1 kg representative material, which was staged crushed to -75  $\mu\text{m}$ . In order to assess whether large PGM were present, two size fractions were created including +38 and -38  $\mu\text{m}$ . The two fractions were then processed using heavy liquids at 2.9 g cm<sup>-3</sup> to remove mainly silicate minerals. The heavy fraction was then processed using a super-panner in order to separate the heaviest (PGM, BMS, BMA) from the lightest (silicates, chromite) minerals (Fig. 3). The processing and recovery of the PGM was carried out at SGS Canada Inc., Canada. The super-panner is designed for small samples and is closely controlled leading to very effective separation. It consists of a tapering triangular deck with a "V" shape cross section (Fig. 3). The table mimics the concentrating action of a gold pan. Initially the sample is swirled to stratify the minerals. Then, the heaviest minerals settle to the bottom and are deposited on the deck surface. In contrast, the less dense material moves towards the top, overlying the heavy minerals. Subsequently, the operation of the deck is then changed to a rapid reciprocal motion, with an appropriate "end-knock" at the up-slope end of the board, and a steady flow of wash water is introduced. The "end-knock" causes the heavy minerals to migrate to the up-slope end of the deck, whereas the wash water carries the light minerals to move to the narrower, down-slope end of the deck.

The heaviest fractions were split into the heaviest fraction (tip) followed by a less dense fraction (middling). One polished section was prepared from each of the heaviest fractions (tip, middling). The results of the PGM recovery are presented as a whole, although the distribution of the PGM was studied on two different size fractions. The concentrates were completely scanned in situ by using a Super Jeol scanning electron microscope (SEM) at the University of Patras. The distribution of the different mineralogical species of the investigated PGM was based on energy dispersive spectrometry (EDS) analyses. The PGM were identified and imaged for area measurements. The area of each PGM was measured in  $\mu\text{m}^2$  and the equivalent circle diameter (ECD: two times the square root of the radius, squared) was calculated.

Quantitative analyses of the PGM were performed at the Department of Earth and Planetary Sciences, McGill University, Canada, using a JXA JEOL-8900L electron microprobe (Jeol, Tokyo) operated in WDS mode at an acceleration voltage of 20 kV and a beam current of 30 nA, with a beam diameter of 2–3  $\mu\text{m}$ . The total counting time was 20 s. The PRZ correction software was used. The X-ray *K $\alpha$*  lines were used for S, As, Fe, Ni, Co and Cu, *L $\alpha$*  lines for Ru, Ir, Rh, Pt and Ag, *L $\beta$*  for Pd and *M $\alpha$*  line for Os and Au. Pure metals were used as standards for all the PGE except Pt for which synthetic PtAs<sub>2</sub> was used, while CoNiAs, native Fe, chalcopyrite, pyrite and PtAs<sub>2</sub> were used as standards for Ni, Fe, Cu, S and As, respectively.

## PREVIOUS WORK ON THE PGM CONTENT OF KORYDALLOS CHROMITITES

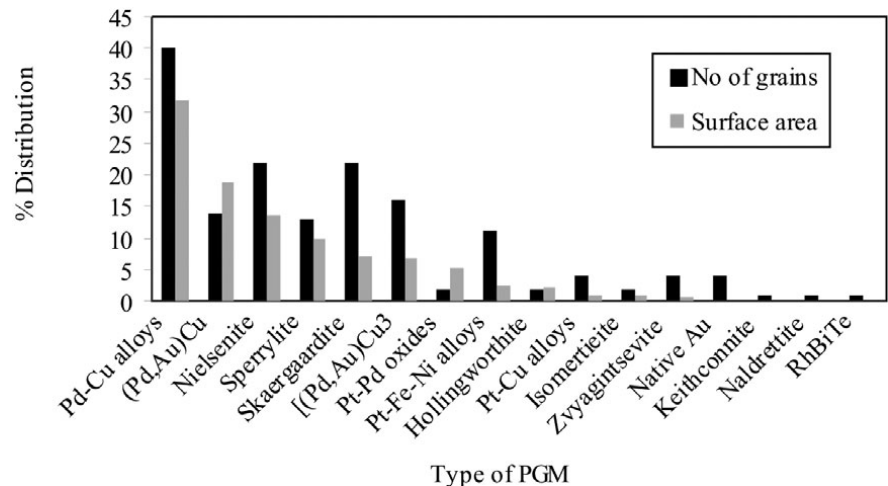
The first data for PGM in the studied chromitites were obtained using the traditionally applied method of the in situ mineralogical investigation (Tarkian et al., 1996; Prichard et al., 2008). The first research carried out by Tarkian et al. (1996) revealed that the PGM assemblage is dominated by three different phases, including laurite (2 grains), sperrylite (2 grains) and an unidentified phase  $\text{Pt}(\text{Ni},\text{Fe})_3$  (4 grains). Laurite (Ru: 36.78–39.81 wt.%, Os: 24.79–27.83 wt.%) was entirely included in chromian spinel, whereas sperrylite and  $\text{Pt}(\text{Ni},\text{Fe})_3$  were found in cracks, along grain boundaries of chromian spinel or in the serpentinized silicate matrix. It was suggested that the majority of the PGM (except for laurite) were of secondary origin based on textural features and appropriate compositional data.

A recent study by Prichard et al. (2008) revealed a more representative PGM assemblage mainly dominated by a Pt-Fe-Ni alloy (over 50 grains), accompanied by a Pd-Pt-bearing alloy (over 30 grains) and sperrylite (9 grains). Moreover, members of the hollingworthite-auriferite-platarsite solid-solution series, laurite, Os-Ir-Ru alloys, Os-Ru-Pt alloys, Pt-Rh alloys, Pt-Cu alloys, Pd-bearing Ni-Fe alloys, and a Pd-Pt-bearing Cu alloy constitute minor phases. The PGM generally range in size from 1 up to 30 x 20  $\mu\text{m}$  in size, are irregular in shape and are located almost exclusively in the altered silicate matrix interstitially to chromian spinel grains, on their edges and in silicate veins cross-cutting chromian spinels. It was proposed that the Pt and Pd minerals were formed as a result of the fractionation of an immiscible sulfide liquid, based on the observation that Pt is commonly associated with Ni-Fe alloys and Pd is alloyed with Cu. Furthermore, it was suggested that the BMA represent sulfide precursors remaining after complete sulfide removal from the monosulfide (mss) and intermediate solid solution (iss) as a result of intensive desulfurization during the

**Table 2** Mineral and distribution % of PGM in the concentrate from the composite sample of Korydallos Al-rich chromitites

PGM TYPE	NO. OF GRAINS	DISTRIBUTION (%)	SURFACE AREA (%) DISTRIBUTION
Pd-Cu alloys	40	25.16	31.61
(Pd, Au)Cu	14	8.81	18.77
Nielsenite	22	13.84	13.62
Sperrylite	13	8.18	9.91
Skaergaardite	22	13.84	7.04
[(Pd, Au)Cu <sub>3</sub> ]	16	10.06	6.77
Pt-Pd oxides	2	1.26	5.13
Pt-Fe-Ni alloys	11	6.92	2.39
Hollingworthite	2	1.26	2.18
Pt-Cu alloys	4	2.51	1.01
Isomertieite	2	1.26	0.93
Zvyagintsevite	4	2.51	0.47
Native Au	4	2.51	0.15
Keithconnite	1	0.63	0.02
Naldrettite	1	0.63	0.01
RhBiTe	1	0.63	0.003
Total	159	100.0	100.00

**Fig. 4** Percentage distribution of different types of PGM in the Korydallos Al-rich chromitites composite sample based on number and surface area of PGM grains.



serpentinization process that affected chromitites.

It is important to note that the above mentioned studies were done exclusively on chromitite samples enriched in PGE (2099–6864 ppb), in which Pt range from 1460 to 4420 ppb. The present study is similarly carried out on such chromitites (also showing Pd enrichment) and a comparison of our results with those of Prichard et al. (2008) is made in order to complete the picture of the controlling factors which are critical with respect to the genesis and mineral processing of the PGM.

## PROCESS MINERALOGY

The dominant minerals in the concentrate by surface area are summarized in Table 2. These include Pd-Cu alloys (31.61%), Pd-bearing tetra-auricupride (18.77%), nielsenite (13.62%), sperrylite (9.91%), skaergaardite (7.04%), Pd-bearing auricupride (6.77%), Pt and Pd oxides (5.13%), Pt-Fe-Ni alloys [including tetraferroplatinum (PtFe), 2.39%], hollingworthite (2.18%) and Pt-Cu alloys [mainly tulameenite ( $\text{Pt}_2\text{FeCu}$ ) and hongshiite (PtCu), 1.01%] (Fig. 4). Isomertieite, zvyagintsevite, native



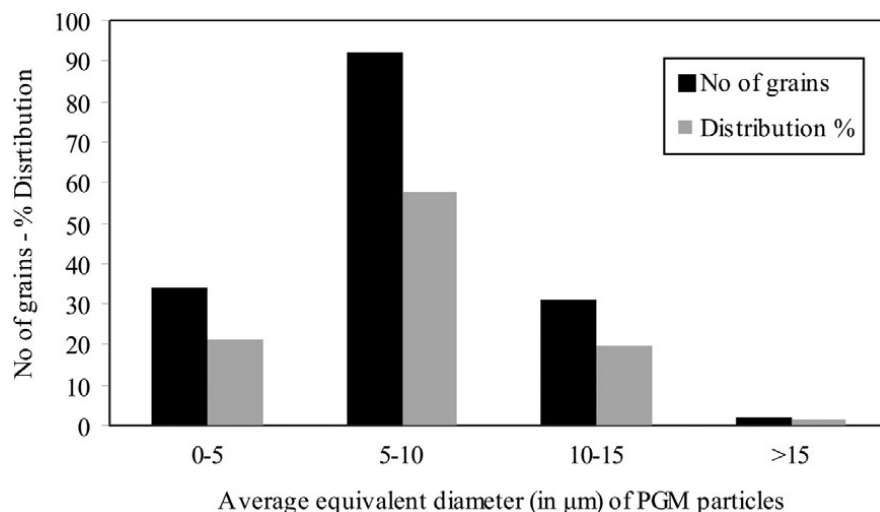


**Fig. 5** Size distribution of PGM in the Korydallos Al-rich chromitites composite sample according to number of PGM grains and percentage of total PGM in each size category.

Au, keithconnite, naldrettite and (cubic, grayish white) Rh-bearing bismuthotelluride constitute minor phases. If the distribution is calculated simply on the number of grains of each mineral phase, then the sample is dominated again by Pd-Cu alloys (25.16%), followed by nielsenite and skaergaardite (13.84%, respectively), Pd-bearing auricupride (10.06%), Pd-bearing tetra-auricupride (8.81%), sperrylite (8.18%), Pt-Fe-Ni alloys (6.92%) and finally by Pt-Cu alloys, zvyagintsevite and native Au (2.51%, respectively). Hollingworthite, isomertieite, keithconnite, naldrettite and Rh-bearing bismuthotelluride are present in small amounts (0.63–1.26%).

The majority of the grains (57.9% or 92 of 159 of the total) are between 5 and 10 µm, 34 grains (21.4%) are less than 5 µm, whereas 33 grains (20.8%) are larger than 15 µm in size (Fig. 5, Table 3). The largest grain is 95 µm across and is composed of Pd-bearing tetra-auricupride and a Pd-rich oxide.

The identified mineral species in both fractions are generally the same, and are dominated by Pd-Cu alloys. However, most of the recovered PGM grains (118 out of 159) are contained in the fine fraction. Pd-bearing tetra-auricupride and Pd-bearing auricupride occur as minor phases in the fine fraction, but constitute the major phases in the coarse fraction. In fact, these Au-based minerals are the dominant phases in the coarse fraction after Pd-Cu alloys. Furthermore, it is noteworthy that single PGM grains are more common in the coarse fraction, and are typically comprised of rich in Au phases.

## PGM CHEMISTRY

Representative electron microprobe analyses of PGM are given in Table 4. These include Pd-Cu alloys that yield the formulae  $\text{Cu}_{0.84}\text{Pd}_{0.15}\text{Ni}_{0.01}$ , and  $\text{Cu}_{0.84}\text{Pd}_{0.14}\text{Pt}_{0.01}\text{Ni}_{0.01}$ , skaergaardite ( $\text{Pd}_{0.90}\text{Au}_{0.06}\text{Fe}_{0.96}\text{Cu}_{0.92}\text{As}_{0.04}\text{S}_{1.04}$ ), nielsenite ( $\text{Pd}_{0.96}\text{Pt}_{0.04}\text{Te}_{0.04}\text{Cu}_{2.92}\text{S}_{2.96}$ ), Pd-bearing auricupride: ( $\text{Au}_{0.72}\text{Pd}_{0.40}\text{Cu}_{2.88}$ ), Pd-bearing tetra-auricupride ( $\text{Au}_{0.60}\text{Pd}_{0.32}\text{Cu}_{1.04}\text{Ni}_{0.02}\text{Fe}_{0.02}\text{S}_{1.08}$ ), sperrylite ( $\text{Pt}_{0.99}\text{Fe}_{0.01}\text{As}_{1.97}\text{S}_{0.02}$ ), and Pt-Fe-Ni alloy  $\text{Ni}_{0.39}\text{Fe}_{0.24}\text{Pt}_{0.22}\text{Cu}_{0.11}\text{Pd}_{0.03}$ . Additional data will be given and discussed in more detail in a paper currently being prepared by the authors.

GRAIN SIZE (µm)	NO. OF GRAINS	DISTRIBUTION (%)
0-5	35	21.4
5-10	92	57.9
10-15	31	19.5
>15	2	1.3
Total	159	100.0

**Table 3** Grain size distribution of PGM in the whole sample of Korydallos Al-rich chromitites

## TEXTURAL AND MINERALOGICAL CHARACTERIZATION OF PGM

The recovered PPGM grains from the Al-rich chromite ores of Korydallos area

occur both as single and polyphase mineral associations, forming anhedral to euhedral grains ranging in size from a few microns up to 95 µm. The composite associations are commonly comprised of different PPGM species or PPGM and BMS or BMA intergrowths. The recovered PGM tend to occur in three different modes, in decreasing order of abundance, as: (i) single or composite inclusions in secondary BMS (mainly millerite) and BMA (mainly awaruite) (Fig. 6a–d); (ii) attachments and epitaxial growths on secondary BMS and BMA (Fig. 6e, f); and (iii) single or composite crystals not related with any altered BM phase (Fig. 6g, h).

Pd-based alloys such as skaergaardite and nielsenite, as well as zvyagintsevite, Pt-Fe-Ni alloys and Rh-bearing bismuthotelluride occur as inclusions in awaruite and millerite (Fig. 6a–d). In these composite PPGM-BM phase microglobules the PPGM tend to occur as irregular aggregates within the BM phase (Fig. 6a) or in the form of droplets (Fig. 6b–d). Some droplet-shaped skaergaardite and nielsenite inclusions may display crystal faces within the secondary BM phases. More than one PPGM species may be found as inclusions in the same secondary BM phase grain (Fig. 6d). Unidentified Pd-Cu alloys, as well as nielsenite and skaergaardite are commonly found as epitaxial growths over awaruite and millerite (Fig. 6e–h), locally accompanied by zvyagintsevite. Pd-bearing tetraauricupride typically forms large crystals (up to 95 µm) (Fig. 6g) and occurs as single-phase grains, and rarely forms intergrowths with Pd-bearing auricupride (Fig. 6h). Sperrylite occurs as subhedral to euhedral grains and is less than 49 µm across. It can also be found in association with nielsenite and isomertieite or with hollingworthite and naldrettite.

It is possible that all the recovered PPGM phases have been affected to some extent by the same secondary process(es) that also caused chromitite hydrothermal alteration. Although it is difficult to determine the degree of PGE mobilization and PGM modification, it is suggested that the recovered PPGM do not represent products of direct

**Table 4** Selected electron microprobe analyses of PPGM from the high-grade PGE Al-rich chromitites of Korydallos area

ANALYSIS	1	2	3	4	5	6	7	8
Wt. %								
Os	—	0.05	—	—	—	—	0.04	0.02
Ir	—	—	—	—	—	—	0.01	—
Rh	—	0.02	—	—	—	—	0.07	0.25
Pt	—	3.14	0.01	2.16	—	0.07	55.91	47.86
Pd	22.64	15.97	53.35	32.37	11.19	15.35	—	3.27
Fe	0.19	0.21	2.46	0.36	0.05	0.29	0.17	14.86
Ni	0.53	1.1	0.11	0.28	0.14	0.32	0.04	25.44
Cu	75.22	78.21	32.97	61.05	50.45	30.61	—	7.81
Au	0.22	0.05	6.98	0.23	37.94	50.39	—	1.06
S	0.07	0.04	0.03	0.03	0.02	0.03	0.23	0.03
As	—	—	1.49	—	—	0.02	42.78	0.04
Bi	—	—	0.06	—	0.1	0.11	—	—
Te	—	0.01	1.67	2.23	0.01	0.03	—	0.07
Pb	0.01	—	0.18	0.11	—	0.17	—	—
Sb	—	—	—	—	0.01	—	0.02	—
Ag	0.06	0.02	0.2	0.03	0.03	0.08	—	—
Total	98.92	98.82	99.51	98.84	99.94	100.46	99.26	100.72
At%								
Os	—	0.018	—	—	—	—	0.024	0.009
Ir	—	—	—	—	—	—	0.004	—
Rh	—	0.016	—	—	—	—	0.083	0.222
Pt	—	1.132	0.004	0.847	—	0.038	32.963	22.13
Pd	15.061	10.555	44.031	23.263	9.589	15.828	—	2.772
Fe	0.237	0.263	3.869	0.49	0.085	0.566	0.342	24.002
Ni	0.638	1.318	0.166	0.365	0.214	0.602	0.078	39.1
Cu	83.803	86.568	45.57	73.476	72.401	52.858	—	11.086
Au	0.08	0.02	3.11	0.09	17.56	29.74	—	0.49
S	0.143	0.094	0.09	0.074	0.057	0.089	0.818	0.096
As	—	—	1.747	—	—	0.026	65.672	0.049
Bi	—	—	0.02	—	0.04	0.06	—	—
Te	—	—	1.15	1.34	0.01	0.02	—	0.05
Pb	—	—	0.08	0.04	—	0.09	—	—
Sb	—	—	—	—	0.01	—	0.02	—
Ag	0.04	0.01	0.16	0.02	0.03	0.06	—	—
Cu#	84.77	89.13	50.86	75.95	88.3	76.96	—	80

—: not detected, analyses 1 to 2: Pd-Cu alloy, 3: Skaergaardite, 4: Nielsenite, 5: Pd-bearing auricupride, 6: Pd-bearing tetra-auricupride, 7: Sperrylite, 8: Pt-Fe-Ni alloy, Cu#: [Cu/(Cu+Pd)]\*100 and atomic formulae.  
 1:  $Cu_{0.84}Pd_{0.15}Ni_{0.01}$ , 2:  $Cu_{0.84}Pd_{0.14}Pt_{0.01}Ni_{0.01}$ , 3:  $(Pd_{0.90}Au_{0.06})(Cu_{0.92}Fe_{0.06}As_{0.04})$ , 4:  $(Pd_{0.96}Pt_{0.04})_{1.00}(Cu_{2.92}Te_{0.04})_{2.96}$ , 5:  $(Au_{0.72}Pd_{0.40})_{1.12}Cu_{2.88}$ , 6:  $(Au_{0.60}Pd_{0.32})_{0.92}(Cu_{1.04}Ni_{0.02}Fe_{0.02})_{1.06}$ , 7:  $(Pt_{0.99}Fe_{0.01})_{1.00}(As_{1.97}S_{0.02})_{1.99}$ , 8:  $Ni_{0.39}Fe_{0.24}Pt_{0.22}Cu_{0.11}$

deposition from hydrothermal fluids. Commonly, secondary PGM alloys are interpreted as resulting from extreme removal of sulfur during serpentinization and/or weathering (e.g. Stockman & Hlava, 1984; Garuti & Zaccarini, 1997). However, all the alloys in the present study are sulfur-free, as indicated by preliminary electron microprobe data. This implies complete desulfurization of

the sulfide precursors or the possibility that they did not form by such secondary processes. In addition, the vast majority of the analyzed PPGM is free of elements such as Sb and Te that are generally interpreted to have been introduced in altered phases via secondary processes (Prichard et al., 1994). Thus, the present data indicate that the recovered alloys were originally

present in the investigated chromitites and do not represent products of hydrothermal or desulfurization processes (e.g. Prichard et al., 2008). However, several features like the presence of nonstoichiometric Pd-Cu alloys strongly support the possibility of their compositional modification.

On the other hand, certain textural and

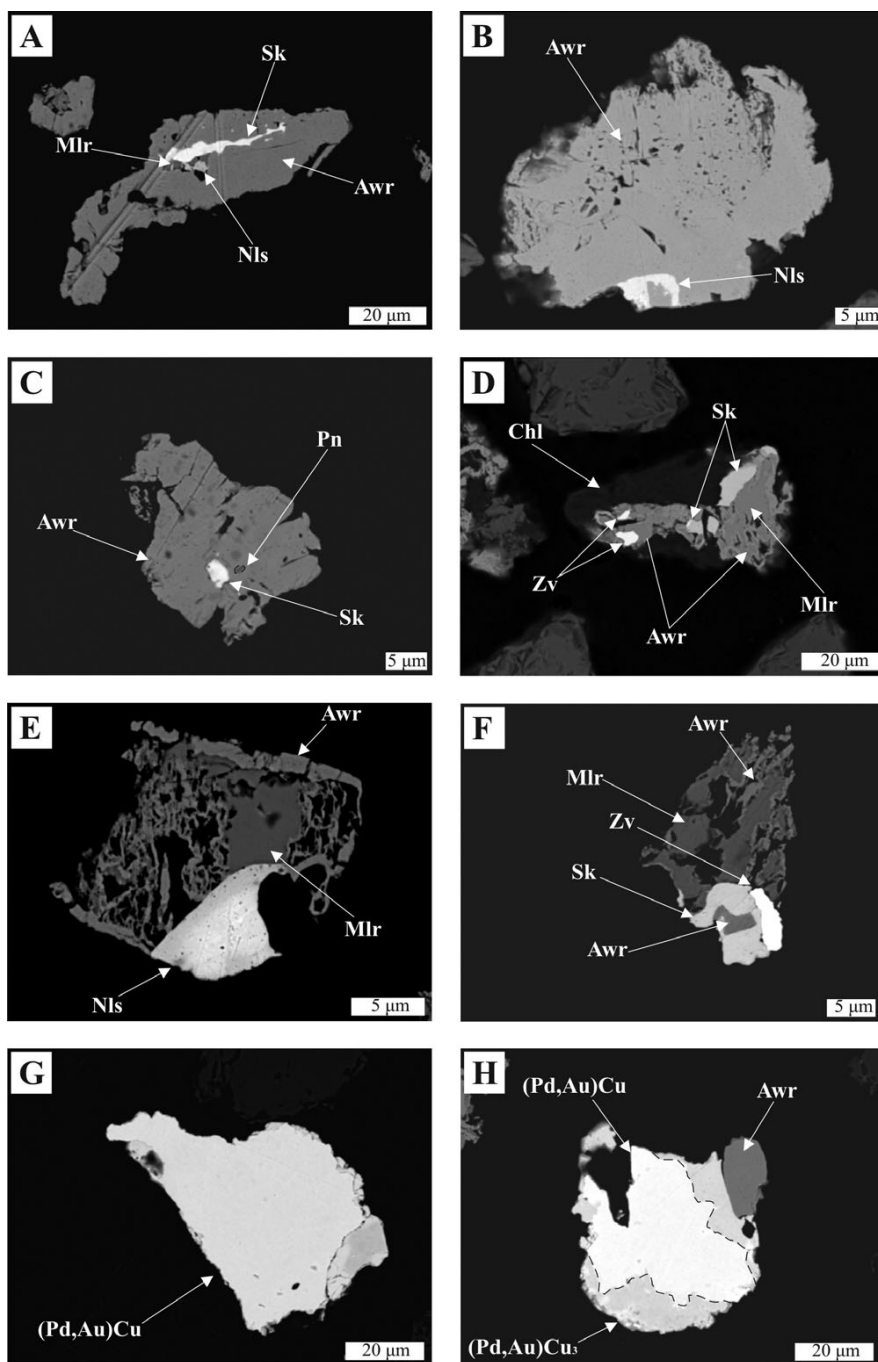


**Fig. 6** Back-scattered-electron microscope images (SEM) showing the morphology, texture and mineral assemblage of the recovered PGM from Korydallos Al-rich chromitites. In pictures C and H the black dashed lines note the presence of pentlandite and the boundary between Pd-bearing tetra-auricupride and Pd-bearing auricupride, respectively. Abbreviations: Sk, skaergaardite; Nls, nielsenite; Awr, awaruite; Mlr, millerite; Pn, pentlandite; Zv, zvyagintsevite; Chl, chlorite.

Pt-Fe-Ni alloys and Pd-bearing tetra-auricupride, respectively, are also interpreted to have a secondary origin as it is the case for PGM oxides from elsewhere (e.g. Garuti & Zaccarini et al. 1997; Proenza et al., 2008).

## DISCUSSION

The present data are important for both petrogenetic studies and for mineral processing purposes. The study of PGM in polished sections usually fails to give the complete picture of PGM paragenesis expected from whole-rock analyses (e.g. Malitch et al., 2003). Additionally, the petrological application of PGE geochemical data should always be used with caution, since they are only indicative and not absolutely representative of the PGE mineralogy (Malitch et al., 2003). In contrast with bulk-rock analytical data and previous studies (Tarkian et al., 1996; Prichard et al., 2008) the recovered PGM assemblage from the investigated chromitites is different, and is mainly dominated by Pd-bearing minerals accompanied by Pt and Au-based phases. The present research yielded a larger number of identified mineral species with a greater grain size variation and occurrence than that from the in situ examination (Tarkian et al., 1996; Prichard et al., 2008). Therefore, it is considered more representative. However, both methodologies, in situ and in-concentrate, are necessary for adequately determining the petrogenetic context of both PGM assemblage and host chromitites. In the present study many minerals previously unknown in the Korydallos chromitites have been discovered (i.e. skaergaardite, nielsenite, Pd-bearing tetra-auricupride, Pd-bearing auricupride, zvyagintsevite, naldrettite, isomertieite, etc.). The PGM assemblage hosted in the examined chromitites is entirely composed of PPGM-based minerals (PPGM), which is quite unusual for mantle hosted ophiolitic chromitites

compositional characteristics are clearly in favor of a secondary origin for specific PPGM. For instance, several Au-Cu and Pd-Cu alloys are chemically zoned. In these grains Pd-bearing auricupride is located around the periphery of Pd-bearing tetra-auricupride (Fig. 6h) and Pd-Cu alloys are surrounded by richer in Cu Pd-bearing alloy phases. The localization of auricupride at the margin of pre-existing tetra-auricupride grains, and thus the increase in Cu content at grain boundaries, are consistent with tetra-auricupride reaction (and replacement) with rich in Cu

hydrothermal fluids. Paragenetically, certain PPGM species are considered to have a secondary origin. For instance, Ramdohr (1967, 1980) considered auricupride to form in hydrothermal veins at temperatures below 390°C. Tulameenite and hongshiite are also considered to have a secondary origin (e.g. Cabri, 1981). Gold occurs in the form of botryoidal strings (up to 10 μm across) in association with Pd-bearing tetra-auricupride, which is indicative of its secondary origin probably after the removal of Au from tetra-auricupride. The Pt- and Pd-bearing oxides accompanying



(e.g. Proenza et al., 2008). However, local Pt and Pd enrichment is known to occur in chromitites from the so-called Moho transition zone and the lower magmatic sequence of some ophiolite complexes (e.g. Bacuta et al., 1990; Lord et al., 1994; Malitch et al., 2003), mainly dependent on the degree of mantle melting (Prichard et al., 1996) and the fertility of the mantle source (e.g. Ahmed & Arai, 2002). Further mineralogical studies are underway in order to correlate the PGE distribution and PGM composition with chromian spinel chemistry, which seem to have significant metallogenic control on the concentration of PGE in ophiolitic chromitites.

In the present study many minerals previously unknown in the Korydallos chromitites have been discovered (i.e. skaergaardite, nielsenite, Pd-bearing tetra-auricupride, Pd-bearing auricupride, zvyagintsevite, naldrettite, isomertieite, etc.). The PGM assemblage hosted in the examined chromitites is entirely composed of PPGM-based minerals (PPGM), which is quite unusual for mantle hosted ophiolitic chromitites (e.g. Proenza et al., 2008). However, local Pt and Pd enrichment is known to occur in chromitites from the so-called Moho transition zone and the lower magmatic sequence of some ophiolite complexes (e.g. Bacuta et al., 1990; Lord et al., 1994; Malitch et al., 2003), mainly dependent on the degree of mantle melting (Prichard et al., 1996) and the fertility of the mantle source (e.g. Ahmed & Arai, 2002). Further mineralogical studies are underway in order to correlate the PGE distribution and PGM composition with chromian spinel chemistry, which seem to have significant metallogenic control on the concentration of PGE in ophiolitic chromitites.

The origin of the primary PGM within chromitites is generally controlled by  $fS_2$ ,  $fAs$  and  $T$  conditions prevailing in the chromitiferous magma (Augé, 1985). The close association of the recovered PPGM with BMS and BMA and the abundance of secondary BM phases in the examined chromitites indicate that an immiscible sulfide melt has been exsolved from the magma

during chromian spinel crystallization in agreement with Prichard et al. (2008). Co-precipitation of chromian spinel and BMS is quite uncommon in ophiolitic chromitites (e.g. Bacuta et al., 1990; Proenza et al., 2001). It probably suggests that it had a significant role in PGE + Au concentration and the final enrichment of these noble metals in the studied chromite deposits. We propose that the majority of PGE + Au were collected by minor amounts of immiscible sulfide droplets formed contemporaneously with and/or after chromian spinel precipitation from a relatively evolved (ultra-)mafic magma. However, it is not clear if the immiscible sulfide melt followed a normal fractionation trend, beginning with a Ni-Fe-rich mss then followed by a Cu-Fe rich iss. The extremely restricted presence of Cu-sulfide relics and the apparent pre-existence of the majority of the recovered PGM alloys bring into question the existence of an initial Ni-Fe-Cu-rich sulfide melt. On the other hand, the possibility that a Pd-Au-Cu alloy melt might have been separated from an initial sulfur-bearing Ni-Fe-Cu melt seems to be more realistic. For instance, Pd-Au-Cu alloys are included in millerite and awaruite in several composite grains, whereas certain PGM alloys such as skaergaardite and nielsenite are intriguingly formed only under conditions of relatively high  $fS_2$  (Rudashevsky et al., 2004; McDonald et al., 2008). Thus, it is plausible that the sulfur-bearing Ni-Fe-Cu melt was locally saturated with a Pd-Au-Cu alloy melt.

The chemically zoned grains of Pd bearing tetraauricupride and Pd-Cu alloys, combined with the presence of PPGM oxides, are direct proof that the PGM assemblage hosted in the chromitites of Korydallos has been modified by secondary processes. The origin of secondary PGM is not yet well understood. The formation of such phases is commonly attributed to post-magmatic processes, which may cover an extended period of time, including ductile asthenospheric and brittle deformation (Tsoupas & Economou-Eliopoulos, 2008), serpentinization/rodingitization, as well as weathering and oxidation processes (e.g. Stockman & Hlava, 1984; Garuti & Zaccarini, 1997;

Zaccarini et al., 2005; Prichard et al., 2008; Proenza et al., 2008; Uysal et al., 2009) under variable climatic conditions. The chemically zoned PPGM are attributed to reaction with a progressively enriched in Cu hydrothermal fluid. However, two different mechanisms have been proposed in order to explain the formation of Pt and Pd oxides (and/or hydroxides): (i) they represent products of the in situ alteration of unstable PGM precursors or (ii) they may precipitate directly from hydrothermal solutions. In the present study the Pt-bearing oxides replace single (nonstoichiometric) Pt-Fe-Ni alloys. The presence of such a Pt-Fe-Ni alloy in a ferrian chromite rim (in situ work) combined with the recovery of several single grains of sperrylite (having almost the same size with Pt-Ni-Fe alloy) are supportive of alloy and oxide formation after complete sperrylite dearsenication followed by oxidation. On the other hand, Pd-bearing tetraauricupride is rarely marginally replaced by Pd-bearing oxides. This suggests that a Cu-rich hydrothermal fluid had the opportunity to transform Pd-bearing tetraauricupride into Pd-bearing auricupride was locally adequately oxidizing to convert tetraauricupride into an oxide phase.

The present data also have metallurgical and economic implications. Most of the PGM are liberated and hence their beneficiation by gravity methods may be an option, especially for high-grade PGE samples. The PGM are effectively concentrated, although losses during beneficiation are expected due to the very fine, locked and discrete PGM grains in chromian spinel and BM phases. Although the PGE grades are high in the Korydallos chromitites, the size of the ore bodies is very small, thus an industrial project is probably not feasible. However, the present study reveals that similar mineral processing and recovery techniques may be put into practice in high-grade PGE, sizeable chromite ores.

## CONCLUSION

The present work has revealed that the PGM data gained by previously carried works based on in situ mineralogical

observations in polished sections and those from the study of concentrated composite chromitite samples are significantly different (i.e. grain size, PGM types, compositional range). Despite the fact that concentrates provide a more representative assessment of the PGE mineralogy, in situ textural information is, however, lost. Therefore, a combined in situ and in-concentrate study is recommended for proper mineralogical characterization even of high-grade PGE rocks and/or ores. Single grain textural information combined with proper statistical evaluation of the mineralogical information, can be proved valuable in explaining the petrological processes responsible for PGE-mineralization. Although the recovery of PGM from high-grade PGE, but small in size chromitite bodies, may not be of a high economic importance, the obtained information may be critical for future and similar, mineral processing projects.

A detailed mineral chemistry study combined with spinel chemistry and geochemistry of chromitites is underway to determine the PGE distribution and PGM petrogenesis and physicochemical conditions of their formation in the area.

## ACKNOWLEDGEMENTS

This paper presents parts of the Ph.D. thesis of A. Kapsiotis at the University of Patras, Greece. We are thankful to Bill Kotsopoulos at the University of Patras for his help with the scanning electron microscope. We would also like to thank Prof J.A. Proenza, two anonymous reviewers for their constructive criticism and helpful comments, and Dr Y. Kajiwara. Research was partly supported by the University of Patras, Karatheodoris Project B097, to TAG. A. Kapsiotis is also thankful to the State Scholarship Foundation of Greece (IKY) for the financial support during his Ph.D. study.

## REFERENCES

- Ahmed, A. H. and Arai, S. (2002) Unexpectedly high-PGE chromitite from the deeper mantle section of the northern Oman ophiolite and its tectonic implications. *Contrib. Mineral. Petrol.*, 143, 263–278.
- Augé, T. (1985) Platinum-group mineral inclusions in ophiolitic chromitite from the Vourinos Complex, Greece. *Can. Mineral.*, 23, 163–171.
- Bacuta, G. C., Kay, R. W., Gibbs, A. K. and Lipin, B. R. (1990) Platinum-group element abundance and distribution in chromite deposits of the Acoje block, Zambales ophiolite complex, Philippines. *J. Geochem. Explor.*, 37, 113–145.
- Cabri, L. J. (1981) Platinum group elements: mineralogy, geology, recovery. *Can. Inst. Min. Met.*, 95–96.
- Cabri, L. J., Beattie, M., Rudashevsky, N. S. and Rudashevsky, V. N. (2005a) Process mineralogy of Au, Pd and Pt ores from the Skaergaard intrusion, Greenland, using new technology. *Miner. Eng.*, 18, 887–897.
- Cabri, L. J., McDonald, A. M., Stanley, C. J., Rudashevsky, N. S., Poirier, B. R., Durham, B. R., Mungall, J. E. and Rudashevsky, V. N. (2005b) Naldrettite Pd<sub>2</sub>Sb, a new intermetallic mineral from the Mesamax Northwest deposit, Ungava region, Québec, Canada. *Mineral. Mag.*, 69, 89–97.
- Capobianco, C. J. and Drake, M. J. (1990) Partitioning of ruthenium, rhodium and palladium between spinel and silicate melt and implications for platinum-group element fractionation trends. *Geochim. Cosmochim. Acta*, 54, 869–874.
- Capobianco, C. J., Hervig, R. L. and Drake, M. J. (1994) Experiments on crystal/liquid partitioning of Ru, Rh and Pd for magnetite and hematite solid solutions crystallized from silicate melt. *Chem. Geol.*, 113, 23–43.
- Economou-Eliopoulos, M. and Vacondios, I. (1995) Geochemistry of chromitites and host rocks from the Pindos ophiolite complex, Greece. *Chem. Geol.*, 122, 99–108.
- Garuti, G. and Zaccarini, F. (1997) In-situ alteration of platinum group minerals at low temperature: evidence from serpentinized and weathered chromitite of the Vourinos Complex, Greece. *Can. Mineral.*, 35, 611–626.
- Grammatikopoulos, T. A., Kapsiotis, A., Zaccarini, F., Tsikouras, B., Hatzipanagiotou, K. and Garuti, G. (2007) Investigation of platinum-group minerals (PGM) from Pindos chromitites (Greece) using hydroseparation concentrates. *Miner. Eng.*, 20, 1170–1178.
- Jones, G. and Robertson, A. H. F. (1991) Tectono-stratigraphy and evolution of the Mesozoic Pindos ophiolite and related units, northwestern Greece. *J. Geol. Soc. Lond.*, 148, 267–288.
- Kapsiotis, A., Grammatikopoulos, T. A., Zaccarini, F., Tsikouras, V., Garuti, G. and Hatzipanagiotou, K. (2006) PGM characterization in concentrates from low grade PGE chromitites from the Vourinos ophiolite complex, Northern Greece. *Appl. Earth Sci. (Trans. Inst. Min. Met. B)*, 115, 49–57.
- Kostopoulos, D. K. (1989) Geochemistry, petrogenesis and tectonic setting of the Pindos Ophiolite, NW Greece. Unpublished Ph.D. Thesis, University of Newcastle, U.K., p. 468.
- Lord, R. A., Prichard, H. M. and Neary, C. R. (1994) Magmatic platinum-group element concentrations and hydrothermal upgrading in Shetland ophiolite complex. *Trans. Inst. Min. Met.*, 103, 87–106.
- McDonald, A. M., Cabri, L. J., Stanley, C. J., Rudashevsky, N. S., Poirier, G., Mungall, J. E., Ross, K. C., Durham, B. R. and Rudashevsky, V. N. (2005) Ungavaite, Pd<sub>4</sub>Sb<sub>3</sub>, a new intermetallic mineral from the Mesamax Northwest deposit, Ungava, region, Quebec, Canada: description and genetic implications. *Can. Mineral.*, 43, 1735–1744.
- McDonald, A. M., Cabri, L. J., Rudashevsky, N. S., Stanley, C. J., Rudashevsky, V. N. and Ross, K. C. (2008) Nielsenite, PdCu<sub>3</sub>, a new platinum-group intermetallic mineral species from the Skaergaard intrusion, Greenland. *Can. Mineral.*, 46, 709–716.
- Malitch, K. N., Junk, S.A., Thalhammer, O. A. R., Knauf, V. V. and Melcher, F. (2003) Diversity of platinum-group mineral assemblages in banded and podiform chromitite from the Kraubath

- ultramafic massif, Austria: evidence for an ophiolitic transition zone? *Mineral. Deposita*, 38, 282–297.
- Melcher, F., Grum, W., Simon, G., Thalhammer, T. V. and Stumpfl, E. F. (1997) Petrogenesis of the ophiolitic giant chromite deposits of Kempirsai, Kazakhstan: a study of solid and fluid inclusions in chromite. *J. Petrol.*, 38, 1419–1458.
  - Migiros, G., Karantasi, S., Kanaki Mavridis, F. and Koronfou Skourtsi, V. (1986) Geological structure of Pindos. IGME [Inst. Geol. Mineral. Explor. (IGME)], Athens, Greece (internal rep.).
  - Pe-Piper, G., Tsikouras, B. and Hatzipanagiotou, K. (2004) Evolution of boninites and island-arc tholeiites in the Pindos ophiolite, Greece. *Geol. Mag.*, 141, 455–469.
  - Prichard, H., Ixer, A., Lord, R. A., Maynard, J. and Williams, N. (1994) Assemblages of platinum-group minerals and sulfides in silicate lithologies and chromite-rich rocks within the Shetland ophiolite. *Can. Mineral.*, 32, 729–746.
  - Prichard, H., Lord, R. A. and Neary, C. R. (1996) A model to explain the occurrence of platinum and palladium-rich ophiolite complexes. *J. Geol. Soc. Lond.*, 153, 323–328.
  - Prichard, H., Economou-Eliopoulos, M. and Fisher, P. C. (2008) Contrasting platinum-group mineral assemblages from two different podiform chromitite localities in the Pindos ophiolite complex, Greece. *Can. Mineral.*, 46, 329–341.
  - Proenza, J. A., Gervilla, F., Melgarejo, J. C., Vera, O., Alfonso, P. and Fallick, A. (2001) Genesis of sulfide-rich chromite ores by the interaction between chromitite and pegmatitic olivinenorite dikes in the Potosí Mine (Moa-Baracoa ophiolitic massif, Eastern Cuba). *Mineral. Deposita*, 36, 658–669.
  - Proenza, J. A., Zaccarini, F., Escayola, M., Cabana, C., Schalamuk, K. and Garuti, G. (2008) Composition and textures of chromite and platinum-group minerals in chromitites of the western ophiolitic belt from Pampeans ranges of Córdoba, Argentina. *Ore Geol. Rev.*, 33, 32–48.
  - Ramdohr, P. (1967) A wide spread mineral association, connected with serpentinization. *Neues Jahrb. Miner. Monatsh.*, 107, 241–265.
  - Ramdohr, P. (1980) *The Ore minerals and their intergrowths*, 2nd edn. Pergamon Press, Oxford.
  - Rassios, A. and Smith, A. G. (2000) Constraints on the formation and emplacement age of western Greek ophiolites (Vourinos, Pindos and Othris) inferred from deformation structures in peridotites. *Geol. Soc. Am. Spec. Pap.*, 349, 473–483.
  - Righter, K., Cambell, A. J., Humayun, M. and Herwig, R. L. (2004) Partitioning of Ru, Rh, Pd, Re, Ir and Au between Cr-bearing spinel, olivine, pyroxene and silicate melts. *Geochim. Cosmochim. Acta*, 68, 867–880.
  - Rudaševskiy, N. S., McDonald, A. M., Cabri, L. J., Nielsen, T. F.
  - D., Stanley, C. J., Kretzer, Y. L. and Rudaševskiy, V. N. (2004) Skaergaardite, PdCu, a new platinum-group intermetallic mineral from the Skaergaard intrusion, Greenland. *Mineral. Mag.*, 68, 615–632.
  - Spray, J. G. and Roddick, J. C. (1980) Petrology and  $^{40}\text{Ar}/^{39}\text{Ar}$  geochronology of some Hellenic sub-ophiolite metamorphic rocks. *Contrib. Mineral. Petrol.*, 72, 43–55.
  - Stockman, H. W. and Hlava, P. F. (1984) Platinum-group minerals in Alpine chromitites from Southwestern Oregon. *Econ. Geol.*, 79, 491–508.
  - Tarkian, M., Economou-Eliopoulos, M. and Sambanis, G. (1996) Platinum-group minerals in chromitites from the Pindos ophiolite complex, Greece. *Neues Jahrb. Miner. Monatsh.*, 4, 145–160.
  - Tsoupas, G. and Economou-Eliopoulos, M. (2008) High PGE contents and extremely abundant PGE-minerals hosted in chromitites from the Veria ophiolite complex, northern Greece. *Ore Geol. Rev.*, 33, 3–19.
  - Uysal, I., Tarkian, M., Sadiklar, M. B. and Sen, C. (2007) Platinum group element geochemistry and mineralogy of ophiolitic chromitites from the Kop mountains, Northeastern Turkey. *Can. Mineral.*, 45, 355–377.
  - Uysal, I., Zaccarini, F., Sadiklar, M. B., Bernhardt, H.-J., Bigi, S. and Garuti, G. (2009) Occurrence of rare Ru-Fe-Os-Ir-oxide and associated Platinum-group minerals (PGM) in the chromitite of Mug̃la ophiolite, SW-Turkey. *N. Jb. Miner. Abh.*, 185/3, 323–333.
  - Whitechurch, H. and Parrot, J. F. (1978) Ecailles métamorphiques infraperidotiques dans le Pindos septentrional (Grèce): croûte océanique, métamorphisme et subduction. *Cr. Acad. Sci. Paris*, 286, 1491–1494.
  - Zaccarini, F., Proenza, J. A., Ortega Gutierrez, F. and Garuti, G. (2005) Platinum group minerals in ophiolitic chromitites from Tehuiztzingo (Acatlan complex, Southern Mexico): implications for post-magmatic modification. *Mineral. Petrol.*, 84, 147–168.
  - Zaccarini, F., Pushkarev, E. V. and Garuti, G. (2008) Platinum group mineralogy and geochemistry of chromitite of the Kluchevskoy ophiolite complex, central Urals (Russia). *Ore Geol. Rev.*, 33, 20–30.



## CONTACT INFORMATION

Email us at [minerals@sgs.com](mailto:minerals@sgs.com)

[WWW.SGS.COM/MINERALS](http://WWW.SGS.COM/MINERALS)

© 2011 SGS. All rights reserved. The information contained herein is provided "as is" and SGS does not warrant that it will be error-free or will meet any particular criteria of performance or quality. Do not quote or refer any information herein without SGS' prior written consent. Any unauthorized alteration, forgery or falsification of the content or appearance of this document is unlawful and offenders may be prosecuted to the fullest extent of the law.